# A theoretical study of ZnCH2 and ZnSnH2 electronic structure and the ZnCH2–HZnCH photolytic rearrangement

**ARTICLE** *in* JOURNAL OF THE AMERICAN CHEMICAL SOCIETY · JANUARY 1996

Impact Factor: 12.11 · DOI: 10.1021/ja951865t



**3 AUTHORS**, INCLUDING:

Miguel San-Miguel
University of Campinas
**53** PUBLICATIONS **739** CITATIONS

SEE PROFILE

Antonio M Márquez
Universidad de Sevilla
**84** PUBLICATIONS **1,338** CITATIONS

SEE PROFILE

# A Theoretical Study of $ZnCH_2$ and $ZnSnH_2$ Electronic Structure and the $ZnCH_2$−HZnCH Photolytic Rearrangement

**M. A. San Miguel, A. Márquez, and Javier Fernández Sanz***

*Contribution from the Departamento de Química Física, Facultad de Química, E-41012, Sevilla, Spain*

*Received June 8, 1995*[⊗]

**Abstract:** A theoretical study of the electronic structure of the prototypical zinc carbenes and zinc stannylenes $ZnXH_2$ (X = C, Sn) as well as their monopositive and dipositive ions $ZnXH_2^+$ and $ZnXH_2^{2+}$ is reported. Based on ab initio Hartree−Fock calculations and introducing electron correlation through second-order Møller−Plesset perturbation theory (MP2), the molecular structures of ground and some excited states of these complexes have been examined. Special attention has been devoted to the analysis of the bond mechanisms between zinc and carbon or tin and how the charge modifies these bonds. Zn−X stretch force constants and dissociation energy profiles are also reported. In the last part of the work an approach to the $ZnCH_2$−HZnCH photolytic rearrangement has been performed. Based on complete active space self-consistent-field (CASSCF) calculations a saddle point on the potential energy hypersurface has been located. A careful analysis of the nature of the wave functions for the 10 lowest states suggests a mechanism involving an excitation toward the first $^3B_1$ excited state lying at 33000 $cm^{-1}$ in agreement with experiment (<35700 $cm^{-1}$).

## 1. Introduction

Transition metal−carbene chemistry has been a topic of growing interest over the last few years mainly due to their putative participation in both organometallic synthesis and homogeneous and heterogeneous catalysis.[1] The nature of the metal−carbon double bond has been the subject of considerable work from both experimental and theoretical viewpoints. Typically, properties of metal−carbon double bonds are rationalized on the basis of two models: Fischer-type complexes or metal−carbenes[2,3] and Schrock-type complexes or metal−alkylidenes.[4] In the Fischer-type complexes the bond corresponds to a $\sigma$-donation/$\pi$-back-donation scheme between the singlet state of carbene and a low-valent transition metal. Schrock-type compounds result when the metal fragment is high-valent, binding then to the carbene in a triplet state.

Among the wide variety of metal−transition carbenes examined up to now, one of the most simple is the zinc carbene $ZnCH_2$. This carbene was isolated in a solid matrix of argon and characterized by infrared spectroscopy (FTIR) by Chang *et al.*[5] in 1987. Besides the general interest of such a prototype molecule, invoked for instance in the mechanism of the Clemmensen reduction,[6] these authors were also able to observe an exciting carbene−carbyne photorearrangement taking place when zinc carbene is irradiated with UV light at $\lambda$ ranging between 280 and 360 nm:

$$ZnCH_2 \xrightarrow[360\text{ - }280\text{ nm}]{UV} HZnCH$$

After this pioneering work, Hamilton and Schaefer reported[7] on an ab initio quantum mechanical study about the molecular structure of zinc carbene and zinc carbyne compounds pointing out that the zinc−carbon bond should be single for carbene and double for carbyne. However, in spite of this progress, some crucial questions concerning the electronic structure and reactivity of these metal−carbon bonds still remain unanswered. First: Do these bonds fit any of the well-established models described above? Second: What is the nature of the bond when the zinc atoms lose their valence electrons giving place to carbenes like $ZnCH_2^{2+}$ in which Zn has its usual oxidation state? Third: What is the mechanism for the carbene−carbyne photolytic rearrangement? To find answers to these questions will constitute an essential part of the present work.

An additional aspect of the problem concerns the possibility of zinc binding heavier group 14 elements. During the last few years the properties of transition-metal silylenes, germylenes, stannylenes, and plumbylenes have received considerable attention.[8] From a theoretical point of view, the nature of transition-metal silylenes has been investigated in the series $MSiH_2^+$ (M = Sc, Ti, V, Cr, Mn, Fe, Co, and Ni).[9] Comparative studies for different group 14 elements have also been reported for Cr and Mo in the $CrXH_2^+$,[9] $(CO)_5MoXH_2$, and $MoXH_2$ series[10,11] (X = C, Si, Ge, and Sn). In the present

[⊗] Abstract published in *Advance ACS Abstracts,* December 1, 1995.

(1) For recent reviews, see: (a) Collman, J. P.; Hegedus, L. S.; Norton, J. R.; Finke, R. G. *Principles and Applications of Organotransition Metal Chemistry*; University Science Books: Mill Valley, CA, 1987. (b) Stephan, D. W. *Coord. Chem. Rev.* **1989**, *95*, 41. (c) Adams, R. D. *Chem. Rev.* **1989**, *89*, 1703. (d) Adams, R. D.; Herrmann, W. A., Eds. The Chemistry of Heteronuclear Clusters and Multimetallic Catalists. In *Polyhedron* **1988**, *7*, 2251. (e) Zanello, P. *Coord. Chem. Rev.* **1988**, *87*, 1. (f) Stone, F. G. A.; Abel, E. W., Eds. *Organometallic Chemistry*; Royal Society of Chemistry: London, 1990; Vol. 18 and earlier volumes.

(2) Fischer, E. O.; Maasbol, A. *Angew. Chem., Int. Ed. Engl.* **1964**, *3*, 580. Fischer, E. O. *Adv. Organomet. Chem.* **1976**, *14*, 1.

(3) For comprehensive reviews, see: (a) Dotz, K. H.; Fisher, H.; Hofmann, P.; Kreissl, F. R.; Schubert, U.; Weiss, K. *Transition Metal Carbene Complexes*; Verlag Chemie: Deerfield Beach, FL, 1984. (b) Cardin, D. J.; Cetinkaya, B.; Lappert, M. F. *Chem. Rev.* **1972**, *72*, 545.

(4) Schrock, R. R. *J. Am. Chem. Soc.* **1975**, *97*, 6577. Schrock, R. R. *Acc. Chem. Res.* **1979**, *12*, 98. Schrock, R. R. *Acc. Chem. Res.* **1990**, *23*, 158.

(5) Chang, S.-C.; Haige, R. H.; Kafafi, Z. H.; Margrave, J. L.; Billups, W. E. *J. Chem. Soc., Chem. Commun.* **1987**, 1682.

(6) Burdon, J.; Price, R. C. *J. Chem. Soc., Chem. Commun.* **1986**, 893.

(7) Hamilton, T. P.; Schaefer, H. F. *J. Chem. Soc., Chem. Commun.* **1991**, 621.

(8) Petz, W. *Chem. Rev.* **1986**, *86*, 1019. Holt, M. S.; Wilson, W. L.; Nelson, J. H. *Chem. Rev.* **1989**, *89*, 11. Herrmann, W. A. *Angew. Chem., Int. Ed. Engl.* **1986**, *25*, 56. Neumann, W. P. *Chem. Rev.* **1991**, *91*, 311.

(9) Cundari, T. R.; Gordon, M. S. *J. Phys. Chem.* **1992**, *96*, 631.

(10) Márquez, A.; Fernández Sanz, J. *J. Am. Chem. Soc.* **1992**, *114*, 2903.

(11) Márquez, A.; Fernández Sanz, J. *J. Am. Chem. Soc.* **1992**, *114*, 10019.

0002-7863/96/1518-0429$12.00/0 

context, the most outstanding difference between carbenes and, for instance, silylenes is based on the relative stability observed for singlet and triplet states. Thus, as is well-known, the triplet $^3B_1$ is the ground state for $CH_2$, the singlet $^1A_1$ lying 9.1 kcal/mol higher;[12] however, this order is reversed for the rest of group 14 homologs, for which the ground state is the singlet and the singlet−triplet splitting increases down the group ($\Delta E_{s-t} = 17-19$,[13], 22,[13a,14] and 24[13a−15] kcal/mol for $SiH_2$, $GeH_2$, and $SnH_2$, respectively). These differences suggest the possibility of a change in the bond mechanism, giving rise to either Fischer- or Schrock-type complexes, depending on the nature of the $XH_2$ group. On the other hand, consideration of structures in which Si, Ge, and Sn are involved in the formation of double bonds leaves open a further question related to the observed trend of such structures to distort. Effectively, theoretical and experimental studies of compounds with these formal double bonds have shown that in the series $Si_2H_4$, $Ge_2H_4$, and $Sn_2H_4$, the planar ethylene-like structure is less stable than the transbent one arising from nonclassical distortion of the double bond.[16−19] Also, in our previous work on the series $MoXH_2$, we were able to show[11] that for the heaviest complex considered, $MoSnH_2$, the structure of the ground state was largely distorted with an out-of-plane angle $\delta$ of 68°:

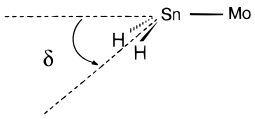


In order to analyze the structural differences between zinc carbene-like complexes $ZnXH_2$, we have considered in the present work the electronic and molecular structure of the heaviest derivative of the series, $ZnSnH_2$, since it is expected that zinc carbene and zinc stannylene will be representative of the limits of behavior (usually plumbylenes are not included in these comparative studies since large spin−orbit effects are expected). The paper is arranged as follows: after a brief computational section, the molecular and electronic structure of $ZnCH_2$ and $ZnSnH_2$ will be carefully examined; then, the properties of cationic species $ZnCH_2^+$, $ZnSnH_2^+$, $ZnCH_2^{2+}$, and $ZnSnH_2^{2+}$ will be considered; finally, a theoretical approach to the photolytic rearrangement carbene−carbyne will be reported.

## 2. Computational Details

Ab initio Hartree−Fock calculations were undertaken using the effective core potential (ECP) reported by Stevens *et al*.[20] to describe inner electrons of zinc and tin atoms. For valence electrons of zinc (3s, 3p, 3d, and 4s) the basis set was (8s8p6d) contracted to [4s4p3d]. For the tin atom, only the 5s 5p electrons were explicitly taken into account following a (5s5p)/[2s2p] contraction scheme. For C and H atoms the standard DZP basis set was used.[21] In most calculations, restricted Hartree−Fock (closed shells) and unrestricted Hartree−Fock (open shells) wave functions were used. Electron correlation was incorporated through second-order perturbational theory under the Møller−Plesset partition (MP2 and UMP2). The calculation of dissociation curves and the photochemical mechanism reported in section 5 were performed by using the complete active space SCF (CASSCF) method.[22] Specific details about the active space will be given there.

The electronic spectrum of $ZnCH_2$ was computed through multireference configuration interaction calculations (MR-CISD) according to a three-class scheme.[23,24] In this procedure, zeroth-order wave functions are determined in a multideterminantal space, the $S_0$ space, and then perturbed by allowing single and double excitations (the P space). The determinants contributing most are incorporated into $S_0$ and the procedure is iterated in order to improve the zeroth-order wave functions. Then, the most significant determinants of P space (the *M* space, ≤20000 determinants) are diagonalized and the variational energies are extrapolated following a procedure close to that proposed by Buenker and Peyerimhoff.[24] The contribution of unlinked clusters is incorporated as proposed by Davidson and Langhoff (MR-CISD+Q).[25]

Molecular geometries were optimized using standard analytical gradients techniques and stationary points were then characterized by computation and further diagonalization of the matrix of second derivatives of the energy $F^x$ in a Cartesian coordinate representation.

All the calculations were performed using GAUSSIAN-92[26] (restricted and unrestricted MP2 optimizations), HONDO-8[27] (CASSCF calculations), and CIPSI[23] (MR-CISD calculations) programs running on a Convex C-240.

## 3. Structure of $ZnCH_2$ and $ZnSnH_2$

The interaction between Zn ground state, $^1S$, and methylene $CH_2$ gives rise to two states depending on whether the latter is triplet or singlet. Geometry optimization leads to a $C_{2v}$ structure for the triplet, state $^3B_1$, which, in agreement with experiment and previous calculations, is the ground state, while the singlet $^1A'$ state shows $C_s$ symmetry and is largely distorted. Structural parameters for both states are reported in Figure 1. Contrary

(12) McKeller, A. R. W.; Bunker, P. R.; Sears, T. J.; Evenson, K. M.; Saykally, R. J.; Langhoff, S. R. *J. Chem. Phys.* **1983**, *79*, 5251. Leopold, D. G.; Murray, K. K.; Stevens Miller, A. E.; Lineberger, W. C. *J. Chem. Phys.* **1985**, *83*, 4849.

(13) (a) Selmani, A.; Salahub, D. R. *J. Chem. Phys.* **1988**, *89*, 1529. (b) Allen, W. D.; Schaefer, H. F. *Chem. Phys.* **1986**, *108*, 243.

(14) Phillips, R. A.; Buenker, R. J.; Beardsworth, R.; Bunker, P. R.; Jensen, P.; Kraemer, W. P. *Chem. Phys. Lett.* **1985**, *118*, 60. Bunker, P. R.; Phyllips, R. A.; Buenker, R. J. *Chem. Phys. Lett.* **1984**, *110*, 351. Pettersson, L. G. M.; Siegbahn, P. E. M. *Chem. Phys.* **1986**, *105*, 355.

(15) (a) Márquez, A.; González, G. G.; Fernández Sanz, J. *Chem. Phys.* **1989**, *138*, 99. (b) Balasubramaniam, K. *Chem. Phys. Lett.* **1986**, *127*, 585.

(16) (a) Trinquier, G.; Malrieu, J. P. *J. Am. Chem. Soc.* **1987**, *109*, 5303. (b) Trinquier, G.; Malrieu, J. P. *J. Phys. Chem.* **1990**, *94*, 6184. (c) Trinquier, G. *J. Am. Chem. Soc.* **1990**, *112*, 2130.

(17) Luke, B. T.; Pople, J. A.; Krogh-Jespersen, M. B.; Apeloig, Y.; Karni, M.; Chandrasekhar, J.; Schleyer, P. v. R. *J. Am. Chem. Soc.* **1986**, *108*, 270. Krogh-Jespersen, K. *J. Phys. Chem.* **1982**, *86*, 1492. Olbrich, G. *Chem. Phys. Lett.* **1986**, *130*, 115. Somasundaram, K.; Amos, R. D.; Handy, N. C. *Theor. Chim. Acta* **1986**, *70*, 393. Teramae, H. *J. Am. Chem. Soc.* **1987**, *109*, 4140.

(18) Trinquier, G.; Malrieu, J. P.; Riviere, P. *J. Am. Chem. Soc.* **1982**, *104*, 4529. Fjeldberg, T.; Haaland, A.; Lappert, M. F.; Schilling, B. E. R.; Seip, R.; Thorne, A. J. *J. Chem. Soc., Chem. Commun.* **1982**, 1407. Nagase, S.; Kudo, T. *J. Mol. Struct. (THEOCHEM)* **1983**, *103*, 35.

(19) Goldberg, D. E.; Hitchcock, P. B.; Lappert, M. F.; Thomas, K. M.; Thorne, A.; Fjeldberg, T.; Haaland, A.; Schilling, B. E. R. *J. Chem. Soc., Dalton Trans.* **1986**, 2387.

(20) Stevens, W. J.; Basch, H.; Krauss, M. *J. Chem. Phys.* **1984**, *81*, 6026. Stevens, W. J.; Krauss, M.; Basch, H.; Jasien, P. G. *Can. J. Chem.* **1992**, *70*, 612.

(21) Dunning, T. H. In *Modern Theoretical Chemistry*; Schaefer, H. F., Ed.; Plenum Press: New York, 1977; Vol. 2. Huzinaga, S. *J. Chem. Phys.* **1965**, *42*, 1293.

(22) Roos, B. O.; Taylor, P. M.; Siegbahn, P. E. M. *Chem. Phys.* **1980**, *48*, 157. Siegbahn, P. E. M.; Almlöf, J.; Heiberg, A.; Ross, B. O. *J. Chem. Phys.* **1981**, *74*, 2384. Roos, B. O. *Int. J. Quantum Chem.* **1980**, *S14*, 175.

(23) Huron, B.; Malrieu, J. P.; Rancurel, P. J. *J. Chem. Phys.* **1973**, *58*, 5745. Evangelisti, S.; Daudey, J. P.; Malrieu, J. P. *Chem. Phys.* **1983**, *75*, 91.

(24) Buenker, R. J.; Peyerimhoff, S. *Chem. Phys.* **1975**, *8*, 56. Buenker, R. J.; Peyerimhoff, S. *Theor. Chim. Acta* **1975**, *39*, 217.

(25) Langhoff, S. R.; Davidson, E. R. *Int. J. Quantum Chem.* **1974**, *8*, 61. Davidson, E. R. In *The World of Quantum Chemistry*; Daudel, R., Pullman, B., Eds.; Reidel: Dordretch, Holland, 1974.

(26) Frisch, M. J.; Trucks, G. W.; Head-Gordon, M.; Gill, P. M. W.; Wong, M. W.; Foresman, J. B; Johnson, B. G.; Schlegel, H. B.; Robb, M. A.; Replogle, E. S.; Gomperts, R.; Andres, J. L.; Raghavachari, K.; Binkley, J. S.; Gonzalez, C.; Martin, R. L.; Fox, D. J.; Defrees, D. J.; Baker, J.; Stewart, J. J. P.; Pople, J. A. Gaussian, Inc.: Pittsburgh PA, 1992.

(27) Dupuis, M.; Chin, S.; Márquez, A. CHEM-Station and HONDO: Modern Tools for Electronic Structure Studies Including Electron Correlation. In *Relativistic and Electron Correlation Effects in Molecules and Clusters*; Malli, G. L., Ed.; NATO ASI Series; Plenum Press: New York, 1994.

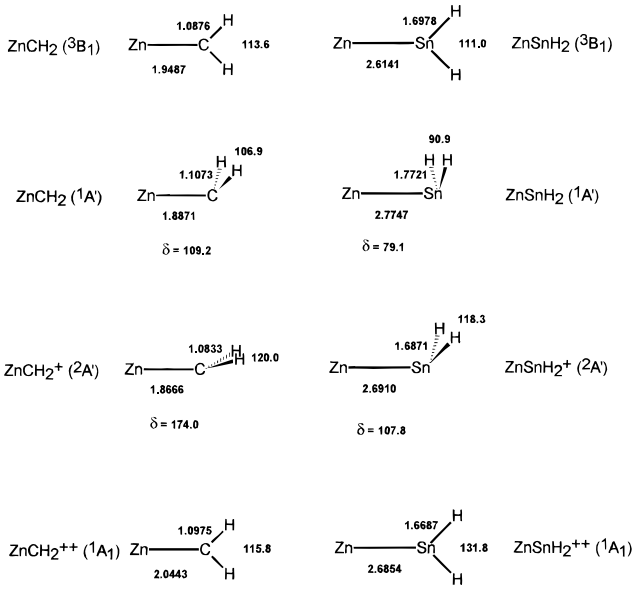


**Figure 1.** Optimized geometries (MP2) of $ZnXH_2$, $ZnXH_2^+$, and $ZnXH_2^{2+}$ (X = C, Sn). For nonplanar geometries $\delta$ refers to the out-of-plane angle. Bond distances in Å and angles in deg.

to the CISD calculations reported by Hamilton and Schaefer,[7] at the MP2 level, the Zn−C bond distance is lower for the singlet than for the triplet although the values agree with the Zn−C interatomic distance observed, for instance, in dimethylzinc (1.93−1.96 Å).[28]

Disregarding the Zn core electrons described by the ECP, the electronic configuration for the triplet is

$$1a_1^2\ 2a_1^2\ 1b_1^2\ 1b_2^2\ 3a_1^2\ 4a_1^2\ 1a_2^2\ 5a_1^2\ 2b_1^2\ 2b_2^2\ 6a_1^2\ 3b_2^2\ 7a_1^2\ 3b_1^1\ 8a_1^1$$

The $4a_1$ and $3b_2$ molecular orbitals (MOs) correspond to the $\sigma_{CH} + \sigma_{CH'}$ and $\sigma_{CH} - \sigma_{CH'}$ combinations of $CH_2$ while $3b_1$ MO corresponds to an almost pure carbon $p_x$ atomic orbital which is not involved in the bond. As can be seen from the MO diagram, Figure 2, interaction between zinc and methylene can be depicted as an overlap between the $sp_\sigma$ MO of $CH_2$ ($3a_1$ MO) and the zinc 4s atomic orbital. This mix corresponds formally to a three-electron/two-center interaction and gives place to $7a_1$ and $8a_1$ MO's. Inspection of the electron density plots for these MO's, Figure 3, confirms the bonding and antibonding character of these MO's as well as the $p_x$ nature of the $3b_1$ MO. Furthermore, it is worth noting that the $8a_1$ MO results from an almost exclusive mix of 4s and $4p_z$ zinc atomic orbitals suggesting that, in localized terms, one lone electron lies above the zinc atom, as confirmed by a spin density population analysis (0.99 electron on Zn). This strong mix between 4s and $4p_z$ atomic orbitals suggests that in fact the dissociation limit for zinc carbene would not be the $^1$S state but the $^1$P one corresponding to a $4s^1\ 4p^1$ atomic configuration. This point can be best understood from the cross-section potential energy hypersurfaces for dissociation of $ZnCH_2$ states reported in Figure 4. In order to ensure correct dissociation, these energy profiles have been obtained from CASSCF calculations where the active space was the Zn 4s and 4p orbitals and the $CH_2$ $sp_\sigma$ and $p_x$ MOs (i.e. 4 electron/6 orbitals). As shown in Figure 4, interaction between Zn($^1$S) and $CH_2$($^3B_1$) would give place to a repulsive curve crossing that arises from the interaction between Zn($^1$P) and $CH_2$($^3B_1$). However, since under $C_{2v}$ constraint both the $^1$S state and the $z$ component of the $^1$P multiplet have $A_1$ symmetry, an avoided cross is observed. In summary, the Zn−C bond in the ground state of zinc carbene can be described as a pairing of the methylene $sp_z$ electron and the $4s4p_z$ zinc one whereas the carbon $p_x$ and the remainder $4sp_z$ electrons are nonbonding

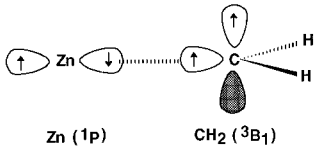


The electronic configuration for the $^1$A′ singlet state is reported in Figure 2. The 5a′ and 4a″ MO's correspond to symmetric and antisymmetric $\sigma_{CH}$ combinations as for the $C_{2v}$ ground state structure. The 9a′ MO is a mix of the $p_x$ methylene MO and 4s and 4p Zn atomic orbitals, as can be seen in Figure 3, where electron density plots for relevant MO's are reported. Finally, the 10a′ MO corresponds almost purely to the $sp_\sigma$ of $CH_2$. The bond in this state can be interpreted then as follows: methylene pyramidalizes and there is a rehybridization of carbon orbitals from $sp^2$ to $sp^3$.

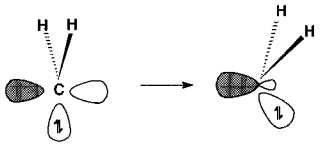


This rehybridization allows the zinc atom to donate the 4s electron pair toward a methylene $sp^3$ orbital while the $sp_\sigma$ electron pair becomes a nonbonding lone pair. This state, on the other hand, dissociates directly to the Zn($^1$S) and $CH_2$($^1A_1$) fragments as shown in Figure 4.

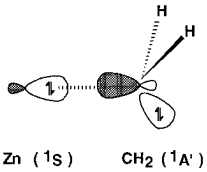


After discussing the nature of the Zn−C bond in both states, we can now compare them and analyze their relative strengths. First of all, it should be noticed that in both cases the bond is formally single and they do not fit any of the limit models sketched in the introduction. In this sense to use the term *carbene* for $ZnCH_2$ complexes is, at the least, unfortunate. On the other hand, computation of Zn−C bond indices[29] at the Hartree−Fock level gives 0.84 for the triplet and 0.96 for the singlet, suggesting that in the latter, the bond mechanism is somewhat more efficient. This idea is confirmed by the values of the stretching force constant $f_{Zn-C}$ computed after a normal coordinate analysis performed using internal symmetry coordinates. At the MP2 level, these force constants are 2.04 and 2.10 mdyn/Å for triplet and singlet states, respectively. Finally, dissociation energies for the Zn−C bond at the MP2 level are estimated to be 28.8 kcal/mol for the triplet and 37.2 kcal/mol for the singlet, also in agreement with a stronger bond in the case of the $^1$A′ state.

The interaction of the zinc atom ($^1$S) with the $SnH_2$ fragment leads to zinc stannylene $ZnSnH_2$, giving rise to triplet and singlet states in a similar way as zinc carbene. However, since for the $SnH_2$ fragment the singlet $^1A_1$ state lies lower than the triplet

(28) Almenningen, A.; Helgaker, T. U.; Haaland, A.; Samdal, S. *Acta Chem. Scand., Ser. A* **1982**, *36*, 159.

(29) Villar, H. O.; Dupuis, M. *Chem. Phys. Lett.* **1987**, *142*, 59 and references therein.

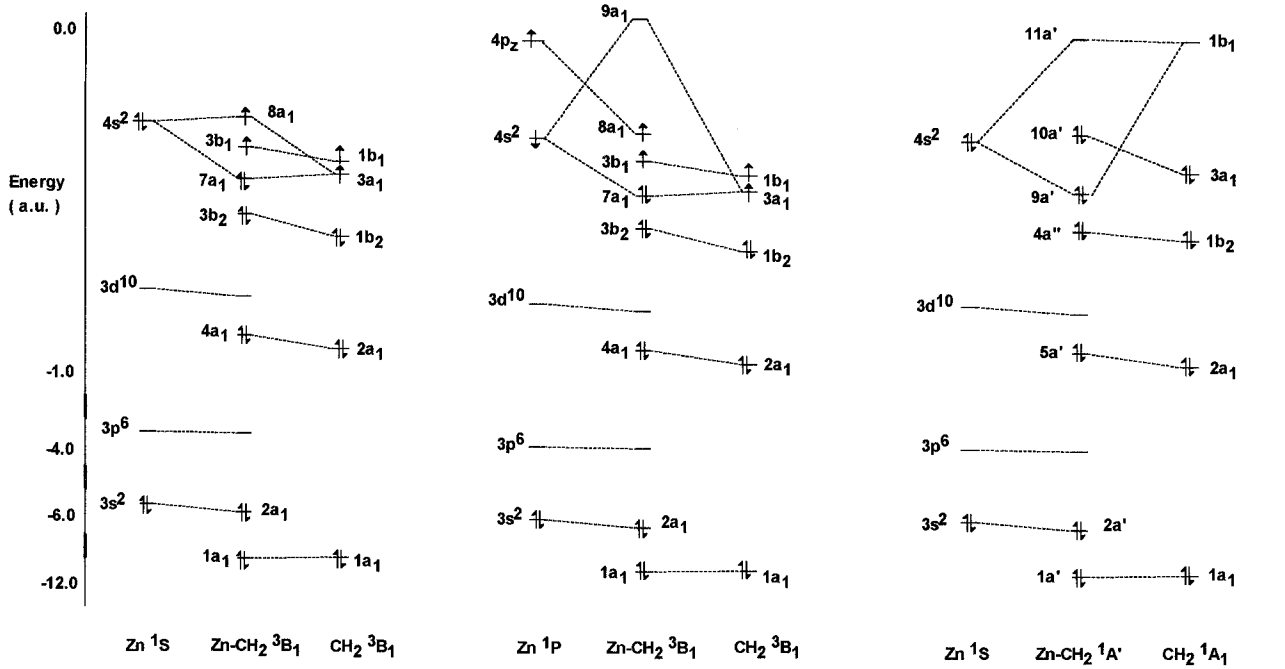


**Figure 2.** Molecular orbital diagrams for $^3B_1$ and $^1A'$ states of $ZnCH_2$: (left) Zn ($^1S$) + $CH_2$ ($^3B_1$), (middle) Zn ($^1P$) + $CH_2$ ($^3B_1$), (right) Zn ($^1S$) + $CH_2$ ($^1A'$).

$^3B_1$, the ground state is expected to be a singlet. Effectively, at the MP2 level of calculation, the $^3B_1$ state of $ZnSnH_2$ falls 16.1 kcal/mol above the singlet $^1A'$. Also, geometry optimization of these states shows $C_{2v}$ symmetry for the triplet and $C_s$ for the singlet although the latter appears to be considerably more distorted than its carbenic homologs. As far as we can ascertain, there are no experimental data on zinc stannylene type compounds; however, the computed Zn−Sn bond distances (2.614 and 2.775 Å at the MP2 level) are in agreement with those computed for other transition metal−tin systems (2.67 Å in $CrSnH_2^+$,[9] 2.80 Å in $MoSnH_2$[11]). The electronic structures of these complexes are fairly close to that of their carbon analogs as can be seen in Figure 6 where orbital diagrams are depicted. For the triplet state, $5a_1$ and $3b_2$ MO's are $\sigma_{CH}$ combinations whereas $3b_1$ corresponds almost purely to the tin $p_x$ orbital. The $6a_1$ MO results from overlap between the $sp_\sigma$ orbital of the $SnH_2$ fragment and the 4s zinc atomic orbital, and the $7a_1$ MO arises from a mix of 4s and $4p_z$ zinc atomic orbitals (see Figure 6 for MO plots). In the case of the singlet $^1A'$ state, there is also a $\sigma$-donation of the Zn $4s^2$ electron pair toward the $SnH_2$ fragment but in a somewhat different way since now the fragment maintains its $sp^2$ hybridization and, therefore, the donation essentially occurs toward a p atomic orbital. This leads to a *non*-Gillespie structure in which the Zn−Sn−H bond angles should be close to 90°. In fact (Figure 1), these bond angles are found to be about 80°:

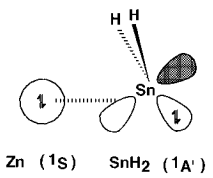


This overbent-type structure has already been observed in sylaketene $H_2SiCO$, for instance, and explained[16a] in terms of an interaction between the $\pi$-type occupied SiH MO and the $\pi^*$ antibonding MO of CO (in our case the $p_z$ orbital of Zn). The difference between the structure of $^1A'$ states of carbon (Gillespie) and tin (non-Gillespie) complexes can be analyzed in a more general context related to nonclassical distortions found in some double bonds in which heavier group 14 elements are involved.[12,16−19] However, in our case the effect is better understood on the grounds of the s−p level splitting instead of the $\Delta E_{S-T}$ gap. Thus, because of the higher split between s and p levels for tin than for carbon, the $sp^2 \rightarrow sp^3$ rehybridization energetic cost is not compensated by the bond stabilization which would result if some mix with the s orbital of tin took place.

Examination of bond indices of $ZnSnH_2$ states shows that, in contrast to $ZnCH_2$, the bond in the singlet is weaker than that in the triplet (0.27 and 0.82 for singlet and triplet, respectively). This fact is confirmed by the lower value of the stretch force constant $f_{Zn-Sn}$: 0.32 mdyn/Å for the singlet and 0.84 mdyn/Å for the triplet at the MP2 level. Finally, the bond dissociation energy appears also to be lower for the singlet than for the triplet (7.8 and 10.3 kcal/mol, respectively, Figure 7).

## 4. Structure of $ZnCH_2^+$, $ZnSnH_2^+$, $ZnCH_2^{2+}$, and $ZnSnH_2^{2+}$

The molecular geometries of the ground state of $ZnCH_2^+$ and $ZnSnH_2^+$ are reported in Figure 1. Both species have $C_s$ symmetry although the tin derivative appears to be much more distorted. Zn−X bond distances are found to be similar to neutral ones but slightly shortened, suggesting a reinforcement of the bond. The electronic structure of charged species can be easily understood from the MO diagram of their respective triplets, Figures 2 and 5. Ionization of $ZnCH_2$ and $ZnSnH_2$ gives place to two doublet $^2A'$ states, and it is worth noting that the lost electron belongs to Zn in the case of carbene, and to Sn in the case of stannylene. This situation agrees with the fact that the first ionization potential of the Zn atom (9.39 eV)[30] is lower than that of $CH_2$ (9.72 eV at the MP2 level) but higher than that of $SnH_2$ (7.15 eV at the MP2 level). Therefore these complexes can be viewed as the interaction of $Zn^+$ ($^2S$) + $CH_2$ ($^3B_1$) for $ZnCH_2^+$ and Zn ($^1S$) + $SnH_2^+$ ($^2A_1$) for $ZnSnH_2^+$. For the carbon derivative, the bond can then be visualized as a pairing of $sp_\sigma$ electrons, the $p_x$ electron remaining as nonbonding. For the tin derivative, there is a donation from the zinc $4s^2$ orbital

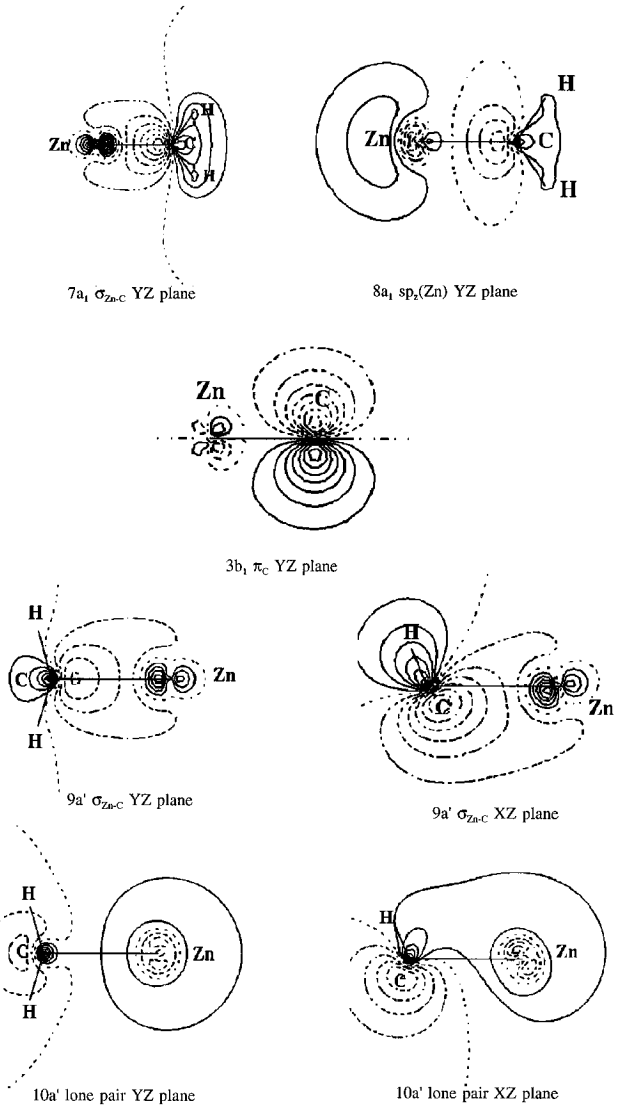


**Figure 3.** Isodensity contours for relevant molecular orbitals of $ZnCH_2$: (top) $7a_1$, $8a_1$, and $3b_1$ MO's of the $^3B_1$ state; (bottom) 9a′ and 10a′ MO's of the $^1A'$ state.

toward an empty tin p orbital while the unpaired tin electron remains as nonbonding. This scheme is similar to that proposed for the $^1A'$ state of $ZnSnH_2$.

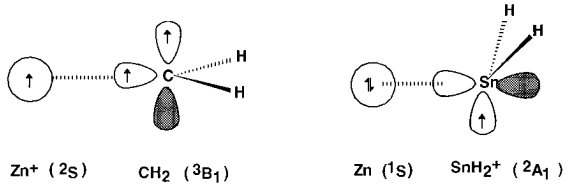


The loss of the $4p_z$ electron for the carbenic compound improves the overlap between zinc and carbon giving a more concentrated and, therefore, stronger bond as confirmed by both the higher dissociation energy (58.1 kcal/mol) and the higher stretch force constant (3.60 mdyn/Å at the UMP2 level). In its turn, the reinforcement of the Zn−Sn bond (D.E. = 29.5 kcal/mol, $f_{Zn-Sn}$ = 0.76 mdyn/Å) can be understood by the lesser repulsion between the tin nonbonding electrons and the zinc cloud.

Let us now consider the structure of dipositive charged complexes $ZnCH_2^{2+}$ and $ZnSnH_2^{2+}$. Geometry optimization shows both compounds to have $C_{2v}$ symmetry and their electronic structure can be understood by a second ionization

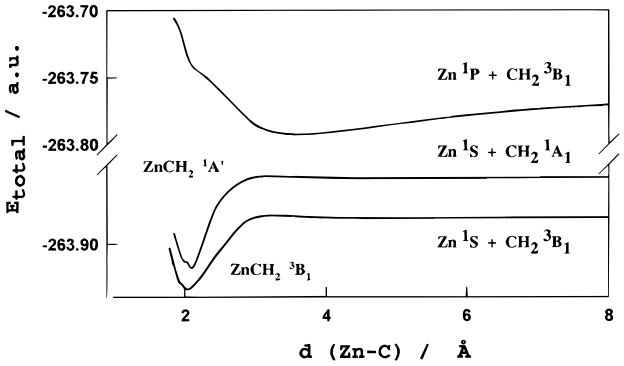


**Figure 4.** Potential energy profiles for dissociation of $ZnCH_2$.

from the neutral complexes (see MO diagrams) or, even better, as a further ionization of monopositive complexes. Care has to be taken, however, in order to deal correctly with the nature of the lost electrons. Starting with $ZnCH_2^{2+}$, ionization of $ZnCH_2^+$ involves the loss of one electron that in principle can be taken out either from $Zn^+$ or $CH_2$ fragments. If the potential ionizations of $Zn^+$ (2nd P.I. of Zn is 17.9 eV[30]) and $CH_2$ (1st P.I. = 9.72 eV at the MP2 level) are considered, it appears that $ZnCH_2^{2+}$ dissociates toward $Zn^+$ ($^2S$) + $CH_2^+$ ($^2A_1$) fragments. However, interaction between these fragments is repulsive and therefore the $ZnCH_2^{2+}$ complex is formed by interaction between $Zn^{2+}$ ($^1S$) and $CH_2$ ($^1A_1$) fragments as shown in Figure 8; although since both curves are of the same symmetry, an avoided cross occurs. With respect to the electronic structure of $ZnSnH_2^{2+}$, ionization of $ZnSnH_2^+$ has to be considered. As already mentioned, the first P.I. of Zn is 9.39 eV while the second P.I. of $SnH_2$ is 14.67 eV (MP2), so $ZnSnH_2^{2+}$ has to dissociate toward $Zn^+$ ($^2S$) + $SnH_2^+$ ($^2A_1$). Again, interaction between these two fragments gives rise to a repulsive curve modified by the avoided crossing with the curve due to the interaction between Zn ($^1S$) + $SnH_2^{2+}$ ($^1A_1$) (Figure 8). In summary, dipositive complexes always result from a stabilizing interaction between neutral and charged species but, depending on the relative P.I. of the fragments, the charged species is $Zn^{2+}$ or $SnH_2^{2+}$. Since $CH_2$ ($^2A_1$) electronegativity is noticeably higher than that of the zinc ion, the bond in $ZnCH_2^{2+}$ should be viewed almost as an ionic pair (in fact Mulliken population analysis shows Zn to bear a net charge of 1.42), and consequently the Zn−C bond strength is expected to be lower than in $ZnCH_2^+$ where a true covalent bond occurs. In the case of the tin complex, Mulliken population analysis reveals that the charge is shared by zinc and tin (net charges are 0.82 and 1.15, respectively) making clear that there is an efficient donation from the zinc atom toward the $SnH_2^{2+}$ fragment. Furthermore, the loss of the nonbonding $SnH_2^+$ electron removes the distorting influence and improves the directionality and, therefore, the overlap, leading to a bond stronger than in the singly charged ion. These ideas are fully confirmed by the trends observed in the Zn−X interatomic distances as well as by the values of the stretch force constants: $f_{Zn-C}$ = 1.73 mdyn/Å and $f_{Zn-Sn}$ = 0.91 mdyn/Å.

## 5. $ZnCH_2$−HZnCH Photolytic Rearrangement

In order to analyze this reaction we will first consider briefly the molecular structure of HZnCH. The optimized molecular structure of this complex shows a linear geometry $C_{\infty v}$. At the UMP2 level the Zn−C, H−Zn, and C−H interatomic distances are found to be 1.864, 1.501, and 1.079 Å, in reasonable

(30) Borg, R. J.; Dienes, G. J. *The Physical Chemistry of Solids*; Academic Press: San Diego, CA, 1992.

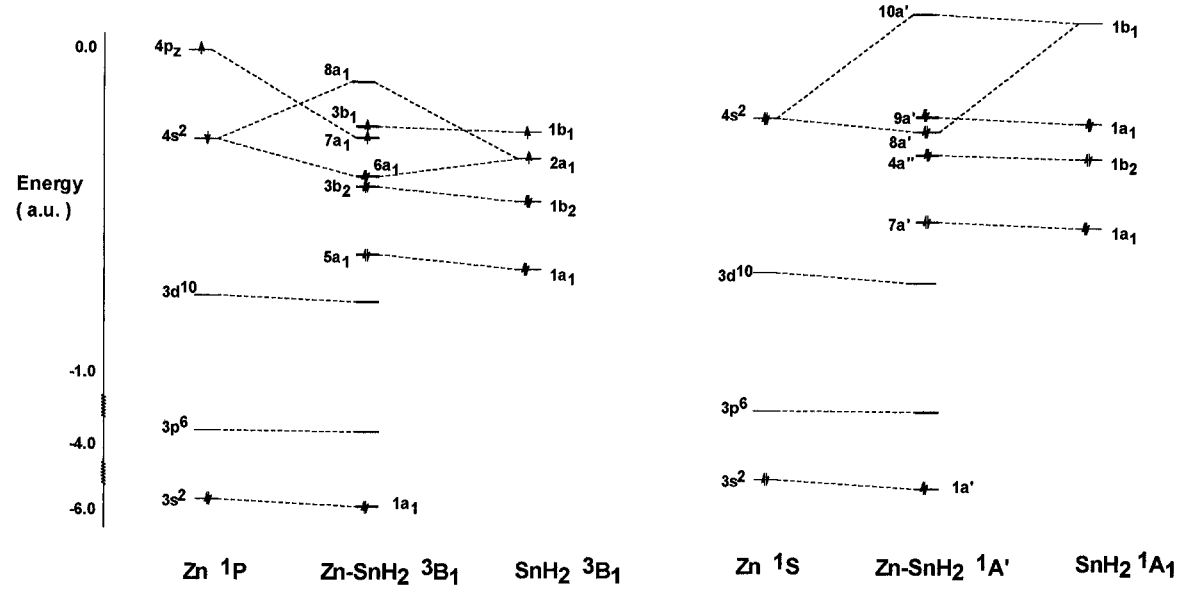


**Figure 5.** Molecular orbital diagrams for $^3B_1$ and $^1A'$ states of $ZnSnH_2$: (left) Zn ($^1P$) + $SnH_2$ ($^3B_1$), (right) Zn ($^1S$) + $SnH_2$ ($^1A'$).

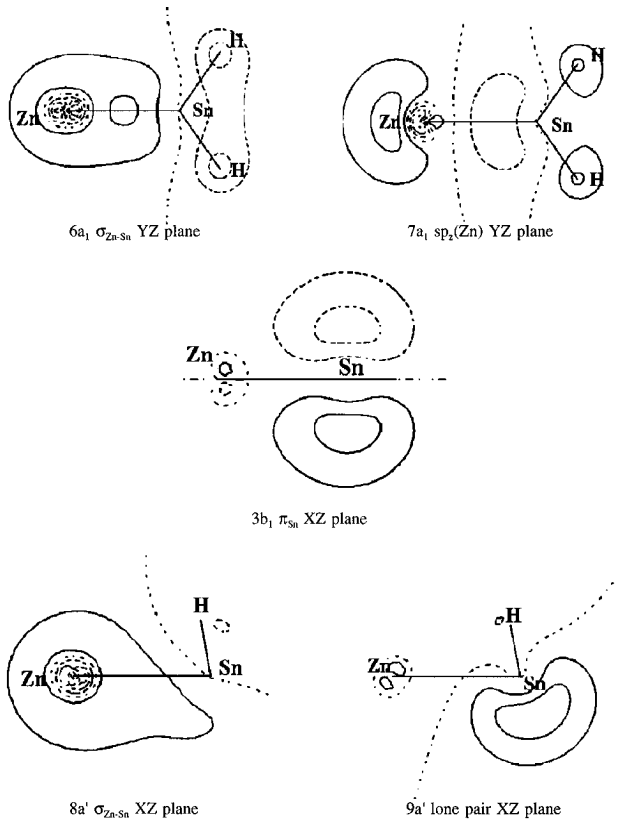


**Figure 6.** Isodensity contours for relevant molecular orbitals of $ZnSnH_2$: (top) $6a_1$, $7a_1$, and $3b_1$ MO's of the $^3B_1$ state; (bottom) 8a′ and 9a′ MO's of the $^1A'$ state.

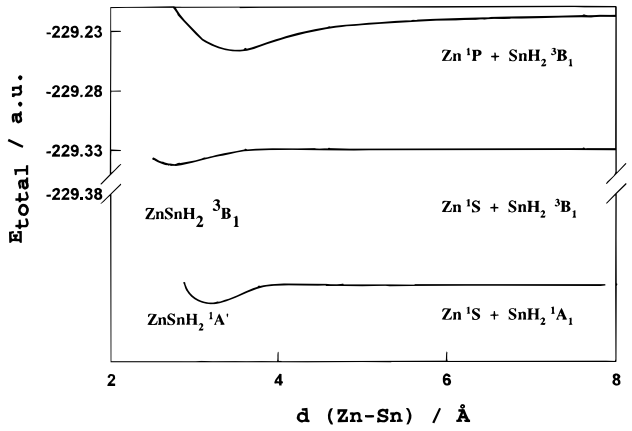


**Figure 7.** Potential energy profiles for dissociation of $ZnSnH_2$.

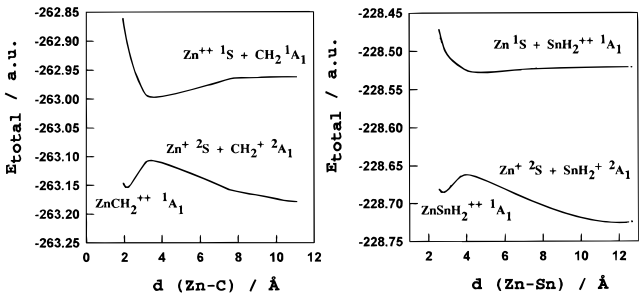


**Figure 8.** Potential energy profiles for dissociation of $ZnCH_2^{2+}$ and $ZnSnH_2^{2+}$.

agreement with the DZP CISD calculations reported by Hamilton *et al.*[7] ($d$(Zn−C) = 1.883 Å, $d$(H−Zn) = 1.521 Å, $d$(C−H) = 1.083 Å). Also in agreement is its relative energy with respect to the ground state of $ZnCH_2$ ($^3B_1$), i.e. the carbene−carbyne reaction energy: $\Delta E = 24$ kcal/mol at the UMP2 level and 21 kcal/mol from CISD calculations. The electronic structure of HZnCH corresponds to a $\pi^2$ configuration (mainly the carbon $p_x$ and $p_y$ orbitals) which, for a triplet arrangement, gives rise to a $^3\Sigma^-$ electronic state.

In the first step of the study, a stationary point on the hypersurface potential energy was determined. These calculations were carried out using CASSCF wave functions in which the active space was the whole valence space with the exception of the Zn $p_x$ orbital which is not expected to be involved in the reaction. In other words, the orbitals in the active space were the two $\sigma_{C-H}$, the $\sigma_{Zn-C}$, and their corresponding antibonding MO's, as well as the carbon $p_x$ and the zinc $p_y$ and $p_z$ orbitals. This 8 electron/9 orbital space resulted in 3696 configuration state functions (CSF) in $C_s$ symmetry. Computation and further diagonalization of the force constant matrix $F^x$ showed that there was only one imaginary eigenvalue whose normal coordinate was associated with the break and formation of the HZn and CH bonds. With the aim of confirming this structure to be the transition state linking carbene and carbyne, the full cross-section curve was computed using the intrinsic reaction coordinate method.[31] The results are summarized in Figure 9. As can be

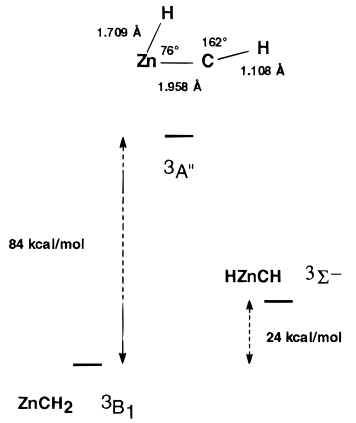


**Figure 9.** Structure of the transition state and relative energies for the zinc carbene−zinc carbyne rearrangement obtained from CASSCF calculations.

**Table 1.** Relative Energies (cm$^{-1}$) for the ZnCH$_2$ Lowest Excited Triplet States of Each Symmetry

| State | $n^a$ | MR-CISD | MR-CISD + Q |
|---|---|---|---|
| $^3B_2$ | 406 | 52673 | 52214 |
| $^3B_1$ | 456 | 33731 | 33183 |
| $^3A_1$ | 363 | 29416 | 29086 |
| $^3A_2$ | 359 | 28078 | 28028 |
| X $^3B_1$ | 456 | 0 | 0 |

[a] *n* refers to the number of determinants in the subspace $S_0$. In the MR-CISD calculations, the mean number of determinants diagonalized in the last step was 15 000 (space *M*). The number of determinants in the *P* space ranged between 22 and 27 million. Through diagonalization, about 70−75% of the perturbational energy was recuperated. The errors in the extrapolation procedure ranged between 0.005 and 0.013.

seen the transition state structure is planar and shows a C−H bond almost broken while the H−Zn bond is practically accomplished (1.709 Å). The barrier was estimated to be 84 kcal/mol, clearly showing that only a photochemical process would be able to produce the reaction.

In order to determine which excited states are well suited for the process, a calculation of some excited triplet states was carried out. These calculations were performed at the multireference configuration interaction (MR-CISD) level using a variational−perturbational iterative procedure according to the CIPSI scheme.[23] Results for the lowest excited states of each symmetry are reported in Table 1. As can be seen, there are three states with transition energies ranging between 28000 and 33000 cm$^{-1}$, while state $^3B_2$ lies at about 52000 cm$^{-1}$ above the ground state. As stated in the introduction section, Chang *et al.*[5] found that the reaction occurred when zinc carbene was irradiated with light of $\lambda \geq 280$ nm, i.e. energy lower than 35700 cm$^{-1}$, therefore the $^3B_2$ state can be ruled out (transitions to $B_2$ states are also symmetry forbidden).

On the other hand, assuming that hydrogen migration occurs in the molecular plane, i.e. $C_s$ symmetry is preserved during the reaction, among the states falling into the experimental range, the $^3A_1$ state can also be discarded. According to group correlation tables, the $\Sigma^-$ species correlates in the $C_s$ group with A″, which, in turn, correlates with $A_2$ and $B_1$ species in the $C_{2v}$ group. In other words, only the $^3A_2$ and $^3B_1$ states would be photochemically active. The lowest one is the $^3A_2$ state (28000 cm$^{-1}$). Analysis of the CI wave function for this state shows that it formally corresponds to a transition from the Zn $p_z$ lone electron toward the Zn $p_y$ atomic orbital (C-$p_x^1$, Zn-$p_y^1$ configuration)

(31) Ishida, K.; Morokuma, K.; Komornicki, A. *J. Chem. Phys.* **1977**, *66*, 2153.

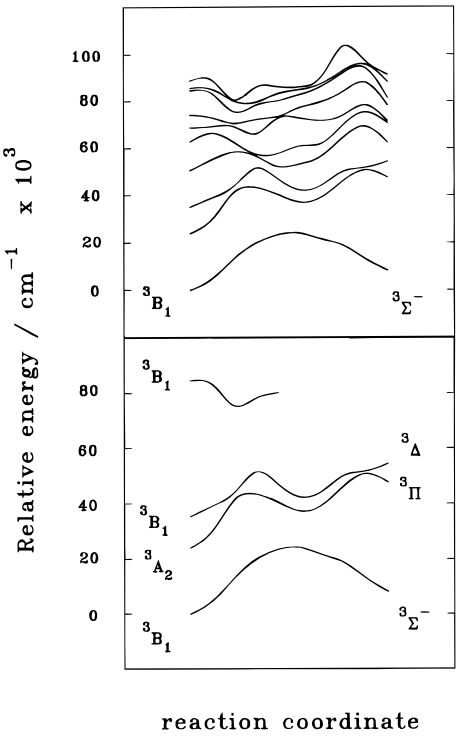


**Figure 10.** Relative potential energy profiles for the carbene−carbyne rearrangement obtained from averaged CASSCF calculations. Bottom: Detail of the excited states involved in the photochemical process. Top: Energies for the 10 lowest triplets $^3A''$ showing the correlation between a $^3B_1$ zinc carbene highly excited state and the $^3\Sigma^-$ zinc carbyne ground state.

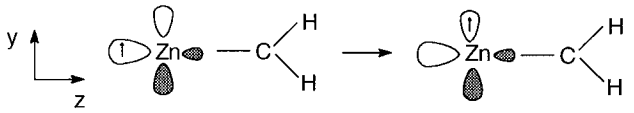


and therefore this state seems to be a good candidate for the reaction since it shows a suitable electronic disposition for a hydrogen transfer from $CH_2$. However, this state shows a considerable energy barrier for the hydrogen migration, and the presence of the $^3B_1$ state just at the height of the barrier precludes invoking an excitation toward a highly excited vibrational level. Instead of that, it seems more likely that the electronic excitation involves the $^3B_1$ state, which along the reaction coordinate mixes, first, with the $^3A_2$ state and, later, with a higher $^3B_1$ state arising from an excitation toward the $\sigma_{CH}$* antibonding MO giving the needed stabilizing component. These ideas are best understood in light of Figure 10 where potential energy curves against the reaction coordinate are plotted for the 10 lowest triplet states of A″ symmetry determined from averaged CASSCF calculations. As can be seen in the lower part, where for simplicity only the relevant states are included, there is, first, an avoided crossing between the states originating from the $^3A_2$ and $^3B_1$ states which then mix with the $^3B_1$ state placed at about 85000 cm$^{-1}$ and which correlates directly with the ground state of products, the triplet $^3\Sigma^-$. The progressive lowering of this $^3B_1$ state along the reaction path is nicely observed at the top of Figure 10.

## 6. Summary and Conclusions

In the first part of this paper ab ab initio study of the electronic structure of prototypical zinc carbenes and zinc stannylenes $ZnXH_2$ (X = C, Sn) has been reported. The ground state of $ZnCH_2$ is found to be the triplet $^3B_1$ in agreement with

experiment[5] and previous calculations.[7] The bond in this complex is easily understood, assuming the participation of the Zn $4s^1$ $4p^1$ configuration, and can then be described as a pairing of $CH_2$ $sp_\sigma$ and Zn $4sp_z$ electrons while the C $p_x$ and the Zn $p_z$ electrons remain as nonbonding. The singlet state of $ZnCH_2$ (11.7 kcal/mol above) features pyramidalization and the bond is described as a $sp^2-sp^3$ rehybridization of $CH_2$ orbitals allowing then the Zn atom to donate its $4s^2$ electrons toward an empty C $sp^3$ orbital.

The electronic structure of $ZnSnH_2$ is closely related to that of $ZnCH_2$, but there are two main differences. First of all, the ground state is not the triplet but the singlet, in agreement with the singlet−triplet splitting of $^3B_1$ and $^1A_1$ states of the $SnH_2$ fragment. Second, because of the higher splitting of atomic tin s and p levels, there is no rehybridization of $sp^2$ orbitals in the $^1A_1$ $SnH_2$ fragment, and the donation of Zn $4s^2$ electrons occurs toward an empty Sn p orbital almost pure. Consequently, this compound is highly distorted with HSnZn angles close to 90°.

The structure of $ZnXH_2^+$ and $ZnXH_2^{2+}$ has also been considered and we have pointed out that a careful analysis is necessary in order to interpret correctly the origin of the lost electrons.

Finally, the reaction mechanism of the zinc carbene−zinc carbyne photorearrangement has been analyzed through CASSCF calculations. First, a saddle point of $C_s$ symmetry has been located on the potential energy surface. Then, on the grounds of symmetry principles together with a comparison between excitation energies and the experimental conditions, a mechanism has been proposed. In this mechanism, the photoactive state would be the first $^3B_1$ excited state which along the reaction path would mix with a state originating from the $^3A_2$ state of carbene which shows a suitable electronic disposition for the rearrangement. A further mix with a higher $^3B_1$ state arising from an excitation toward a $\sigma^*_{CH}$ orbital would give the needed stabilizing component.

**Acknowledgment.** This work was supported by the DGICYT (Spain, Project No. PB92-0662) and by the European Commission (Contract No. ERBCT1-CT94-0064).

JA951865T